4-14-2017

Investigating Nucleostemin's Regulatory Role in Ribosome Biogenesis

Meghan F. Monroy
University of Connecticut - Storrs, meghan.monroy@uconn.edu

Investigating Nucleostemin's Regulatory Role in Ribosome Biogenesis

Meghan Monroy

B.S. University of Connecticut, 2014

A Thesis

Submitted in Partial Fulfillment of the

Requirements for the Degree of

Master of Science

At the

University of Connecticut

2017

APPROVAL PAGE

Master of Science Thesis

Investigating Nucleostemin's Regulatory Role in Ribosome Biogenesis

Presented by

Meghan Monroy, B.S.

Major Advisor _____

Victoria Robinson, Ph.D.

Associate Advisor _____

Nathan Alder, Ph.D.

Associate Advisor_____

James Cole, Ph.D.

University of Connecticut

2017

Table of Contents

Introduction

The Nucleostemin (NS) family of guanine nucleotide binding proteins (G-proteins) is well conserved in Eukaryotes[23]. The family includes the vertebrate paralogs G-protein nucleolar 3 like (GNL3L) and G-protein nucleolar 3 (GNL3), and the shared invertebrate ortholog nucleostemin 1 (NS1) in *Drosophila melanogaster*[23]. The NS family is part of the larger group YlqF Related GTPases (YRG) based on their common ancestor[23]. Evolutionarily, the YRG proteins have played a role in ribosome biogenesis and regulation[23]. GNL3 took on additional roles, such as the regulation of cell cycle progression, when it genetically diverged from its parental GNL3L gene in vertebrates[39].

NS protein family members are found in the nuclear compartment of the cell where they shuttle between the nucleoplasm and the nucleolus in a GTP-dependent manner[29]. This trafficking is facilitated by the GTPase activity of the circularly permuted GTPase (cpGTPase) domain located in the center of these proteins[5,29]. G-motifs (G1, G2, G3, G4 and G5) are highly conserved amino acid sequences that delineate the guanine nucleotide-binding site of the protein and, therefore, identify members of the G-protein superfamily[35]. Unlike canonical GTPases, the cpGTPase G-motifs are ordered where G4 and G5 precede G1, G2 and G3 (Figure 1)[1]. The functional consequences of this re-ordering are poorly understood, however, cpGTPases likely maintain the same structural fold as canonical GTPases as suggested by the X-ray crystallography structures of the bacterial cpGTPases, YlqF and YjeQ[13,17,33].

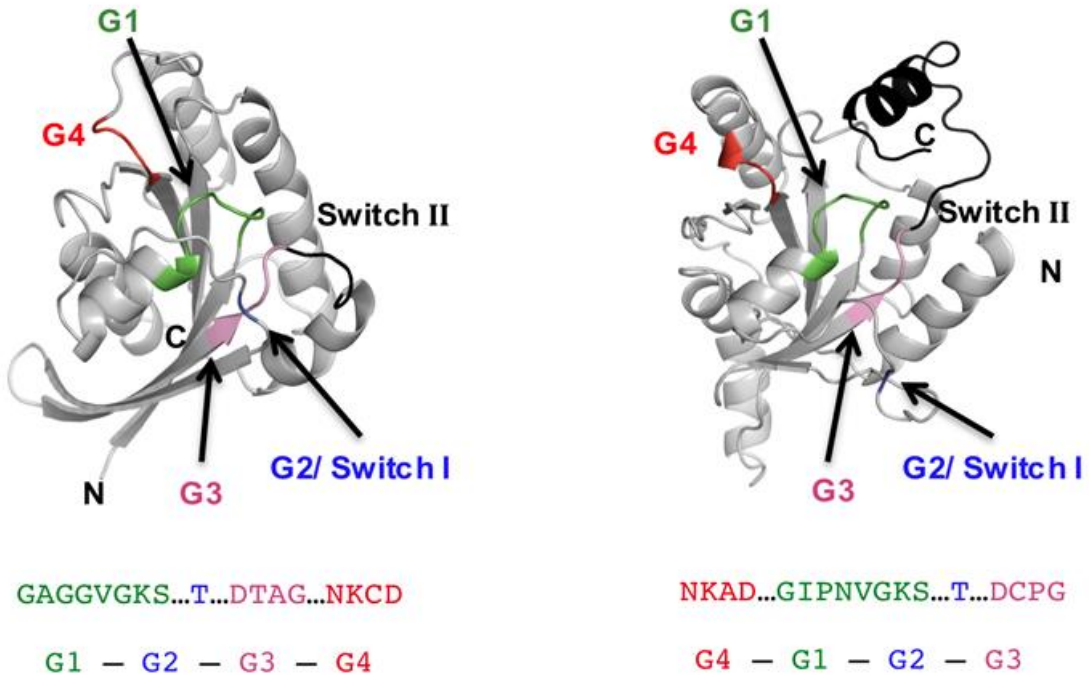

Figure 1. A. Structural comparison of canonical and circularly permuted GTPases. Ribbon diagram and amino acid sequence of the X-ray crystallography structure of HRAS showing the G-domain order of a canonical GTPase[25]. **B.** Ribbon diagram and amino acid sequence of a predicted structure of NS1 showing the G-domain order of a cpGTPase. The X-ray crystallography structure of YlqF was used to generate the I-TASSER homology model (Tyler Daman, *unpublished*)[13,42].

Interactions with cellular partners also regulate the nucleolar localization of various NS family members. For example, GNL3L binds TRF1 in the nucleoplasm to promote telomeric association with TRF1[43]. Another nucleolar binding partner of GNL3L is MDM2, which regulates p53 activation[22]. These studies implicate NS in cell cycle progression. GNL3 interacts with Nucleophosmin (NPM), a nucleolar phosphoprotein that is involved in rRNA processing, and ribosome assembly[21]. Recent structural studies from our group reveal that the N- and C-terminal regions of these proteins are intrinsically disordered (IDR) (Tyler Daman, *unpublished*). IDRs are defined by the lack of secondary and tertiary structure, which is important for recognition of multiple binding partners[40]. The increased flexibility of IDRs provides them with the ability to fold into various conformations depending on the binding event[26].

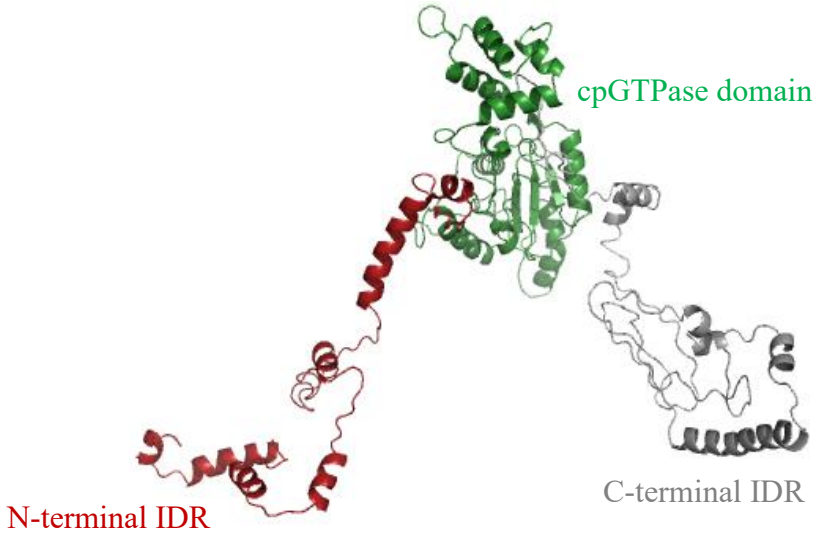

Figure 2. Homology model of the intrinsically disordered regions of NS1. A ribbon diagram of NS1 showing the well-folded cpGTPase domain and the flexible N- and C- terminal IDRs. The X-ray crystallography structure of YlqF was used to generate this I-TASSER homology model (Tyler Daman, *unpublished*)[13,42]

Our lab has been studying *D. melanogaster* NS1 to try to understand how the structural and biochemical properties of this protein contribute to its cellular function. In collaboration with Dr. Patrick DiMario at Louisiana State University, we showed that in *D. melanogaster*, NS1 enriches in the granular components (GC) of nucleoli and is required for maturation and release of the large (60S) ribosomal subunit from nucleoli[30]. These data imply NS1 interacts with one or more components of the ribosome. YlqF and YjeQ also have cellular roles in ribosome biogenesis[11,19]. YlqF binds to the central protuberance (CP) and helps orient the rRNA of the 50S particle[19]. YjeQ is an assembly factor in the later steps of 30S particle maturation of the 70S ribosome[11]. The binding site of YjeQ suggests a chaperone-like role for the 16S rRNA[11]. A major goal of this work then is to determine if NS1 interacts with proteins from the large ribosomal subunit, thereby supporting its role in the structuring and trafficking of the 60S ribosomal subunit.

The nucleolus is a membrane-less organelle within the nucleus where ribosome biogenesis occurs[24,27]. Various pieces of the ribosome are then shuttled from the nucleus to the cytoplasm where the mature 80S ribosome is assembled. The Eukaryotic ribosome is an enormous cellular machine consisting of a small (40S) and a large (60S) subunit coming together to form the 80S species[41]. The megadalton complex contains seventy-nine proteins and four rRNAs, the 18S, 5.8S, 25S, and 28S rRNAs[41]. Cells expend a large amount of energy and resources on maintaining and regulating ribosome synthesis. When the production of ribosomes is halted by a cytotoxic or genotoxic stimuli the cell enters a state of stress, which affects cell cycle progression and promotes tumorigenesis[14].

The multi-step process of ribosome biogenesis involves more than two hundred assembly factors and more than seventy-five small nucleolar RNAs (snoRNA)[14]. In yeast, the 90S pre-ribosome, including the 5S rRNA and the immature 35S pre-ribosomal RNA (pre-rRNA) is generated in the nucleolus (Figure 3). The processing of these pre-rRNAs, mainly by co- and post-transcriptional processing pathways, leads to the formation of a 27S pre-rRNA, which ultimately becomes the 60S particle[14]. A critical step in 35S pre-rRNA processing is the incorporation of the 5S rRNA into the complex with ribosomal proteins L11 (rpL11) and L5 (rpL5) to form the central protuberance (CP)[14]. Following the CP formation, the 66S particle enters the nucleoplasm where maturation of the 60S subunit continues (Figure 3)[14]. Although the function of the 5S ribosomal ribonucleoprotein (rRNP) complex is not fully understood, some studies suggest rpL11 interacts with the P-site bound tRNA facilitating communication between the tRNA and the 5S rRNA for regulation between the P/P and P/E states[6]. Evolutionarily conserved 80S assembly pathways have been shown in other organisms such as *Xenopus laevis*,

mouse and humans[9]. The one documented difference is in humans where the maturation of the 60S particle is postulated to occur in the cytoplasm[9].

The 35S rRNA processing, including the formation of the CP is necessary for the pre-60S ribosomal subunit to continue along the synthesis pathway. Knocking out expression of Grn1p (Δ*Grn1p*), the fission yeast cpGTPase homolog of GNL3L, causes irregular cell growth and an accumulation of pre-ribosomal factors in the nucleoluos[7]. In Δ*Grn1p* cells, GNL3L can rescue 35S pre-RNA processing, nuclear export of ribosomal protein L25a (rpL25a) and cell proliferation[7]. Therefore, Grn1p and GNL3L are required for proper pre-rRNA processing during ribosomal assembly[7]. Similarly, mutations in the 5S rRNP complex lead to a build-up of pre-60S particles in the nucleolus interrupting the production of ribosomes[14]. As stated previously, our study with the DiMario lab examined how a decrease in the expression of NS1 in *D. melanogaster* (by siRNA knockdown) influenced rpL11[30]. We observed an excess of free rpL11 in the nucleolus and a reduction in cytoplasmic ribosomes[30]. When NS1 is not present, rpL11 does not incorporate into the 5S rRNP complex halting 35S pre-rRNA processing. Although NS proteins can transit within the nucleus, they predominantly reside in the nucleolus[27]. Therefore, one explanation for this is that NS1 interacts with rpL11 in the nucleolus, sequestering it so that it becomes incorporated into 60S subunits. When rpL11 is not in the correct cellular location, mature 60S ribosomes are unable to form.

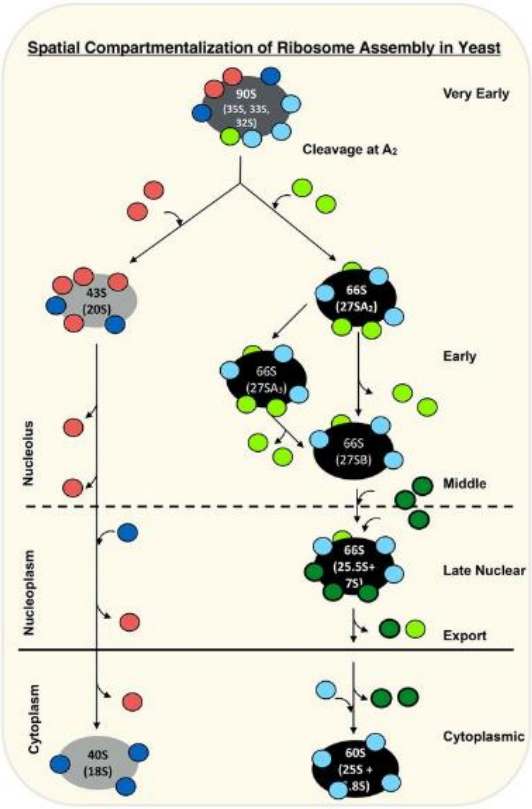

Figure 3. Depiction of the cellular location of 60S subunit assembly. Each pre-ribosomal particle is comprised of pre-rRNA, ribosomal proteins and dynamic assembly factors. The 90S pre-ribosome including the 5S rRNA and the 35S pre-rRNA is generated in the nucleolus. The 90S is processed into a 27S pre-ribosome before the pre-60S particle exits the nucleolus (Adapted from Konikkat, et al.)[14].

This study set out to investigate any potential interactions between NS1 and rpL11 based on their suggested involvement in ribosomal subunit assembly mentioned above. Because rpL11 is associated with several ribosomopathies, our data has implications for finding cures for diseases and cancers that result from improper production of ribosomes[2].

Materials and Methods

Protein Expression

The cDNA of *Drosophila melanogaster* ribosomal protein L11 isoform A (gene ID 37235, *Drosophila* Genomics Resource Center, Bloomington, NJ) was cloned into pET21a and

pET28a expression vectors using FastCloning[18]. In brief, the cDNA and vectors were individually amplified by polymerase chain reaction (PCR) using the primers listed in Table 1. The vector and insert were digested at a 2:1 vector/insert ratio with DpnI for 1 hr at 37 °C. The mixture was used to transform chemically competent *Escherichia coli* DH5α cells. Transformants were selected for with either ampicillin or kanamycin. Colony PCR was performed on several single colonies using T7 primers to determine which cells contained the correctly sized product. Plasmids from those cells were purified using the Promega PureYield Plasmid MiniPrep System. Plasmids were confirmed by sequencing (GeneWiz).

The *D. melanogaster* nucleostemin isoform 1 (gene ID 42060) vectors used in these studies were made by Tyler Daman (Table 2).

NS1 and rpL11 proteins were expressed in Rosetta 2(DE3)pLysS *E. coli* cells (Novagen). The cells were cultured in auto-induction media (1 L) at 37°C until mid-log, at which point the temperature was dropped to 18 °C[34]. The cells were grown for 20 hr and harvested by centrifugation. The cell pellets were stored at -20 °C.

Table 1: Primers Used in Cloning

Protein	Primer Sequence	Size (bp)
rpL11	For 5'-GGTATAGGATCCATGGCGGCGGTTACCAAGAAGATTAAGCGCGAT-3' Rev 5'-CTTGTCGACGGAGCTACTTCTTGGTGTTCAAGATGATACCATCGTA-3'	45 46
T7	For 5'-TAATACGACTCACTATAGGG-3' Rev 5'-GCTAGTTATTGCTCAGCGG-3'	20 20

Table 2: List of Plasmids

Plasmid	Gene Encoded	Vector Backbone
pMM005	rpL11	pET28a
pMM006	rpL11	pET21a
pTD001	NS1	pET21a
pTD046	NS1 1-135	pET21a
pTD052	NS1 490-581	pET28a

Protein Purification

All un-tagged proteins were purified at 4 °C using a purification scheme similar to the one outlined below. The buffers are described in Table 3. It should be noted that NS1 and rpL11 have pIs of 9.4 and 10.1, respectively. The frozen cell pellets were thawed, resuspended in SP A buffer containing 1 mM phenylmethane sulfonyl fluoride (PMSF). Cells were sonicated (Misonix Sonicator 3000) on ice for 6 min in 30 sec intervals at an output level of 4.5. The cell lysate was clarified by centrifugation at 30,000 *x g* for 30 min and loaded onto a 10 mL HiTrap SP FF cation exchange column (GE LifeSciences). Proteins were eluted with a 400 mM to 1 M KCl gradient. Fractions containing either NS1 or rpL11 were identified using sodium dodecyl sulfate-polyacrylaminde gel electrophoresis (SDS-PAGE), pooled, filtered and loaded onto a 15 mL ceramic hydroxyapatite (CHT-I) column (Bio-Rad). A 50 to 600 mM phosphate gradient was applied to the column. As before, fractions containing either NS1 or rpL11 were identified using SDS-PAGE, pooled, concentrated using an Amicon Ultra-15 Centrifugal filter (EMD Millipore) and subject to gel filtration using a Superdex 200 gel filtration column (GE LifeSciences). Fractions corresponding to the monomeric species of each protein (i.e. molecular weight of 21.3 kDa for rpL11 and 65.9 kDa for NS1) were collected and their concentration was determined using the Pierce 660 nm Protein Assay (ThermoFischer Scientific). Samples were flash frozen in liquid nitrogen and stored at -80 °C.

The N-terminal hexa-His tagged proteins were purified using a 10 mL HisTrap FF Crude nickel column (GE LifeSciences) followed by the CHT-I and gel filtration columns in a manner similar to that described above. Buffers for this purification are also listed in Table 3.

Table 3: Purification Buffers

Buffer Name	Buffer Composition	Corresponding Column
SP A	20 mM Tris, 400 mM KCl, 1% glycerol, 1 mM DTT, pH 7	10 mL HiTrap SP FF cation exchange
SP B	20 mM Tris, 1 M KCl, 1% glycerol, 1 mM DTT, pH 7	10 mL HiTrap SP FF cation exchange column
His Binding	50 mM imidazole, 500 mM KCl, 1% glycerol, 20 mM Tris, 1 mM DTT, pH 7	10 mL HisTrap FF crude nickel column
His Elution	500 mM imidazole, 500 mM KCl, 1% glycerol, 20 mM Tris, 1 mM DTT, pH 7	10 mL HisTrap FF crude nickel column
CHT A	50 mM KH_2PO_4, 50 mM K_2HPO_4, 150 mM KCl, 1% glycerol, 1 mM DTT, pH 7	15 mL ceramic hydroxyapatite
CHT B	600 mM KH_2PO_4, 600 mM K_2HPO_4, 150 mM KCl, 1% glycerol, 1 mM DTT, pH 7	15 mL ceramic hydroxyapatite
Gel Filtration	20 mM Tris, 250 mM KCl, 1% glycerol, 1 mM DTT, pH 7	Superdex 200 gel filtration

Pull-Down Assay

The interaction between NS1 and rpL11 was probed using a modified version of a pull-down assay based on affinity chromatography[32]. Assays were done at 4 °C. One mL of an N-terminal His-tag fusion protein (bait protein) at 10 µM was loaded onto a 1 mL HisTrap FF Crude column (GE LifeSciences) and incubated for 15 min to ensure its immobilization to the Ni Sepharose resin. The column was washed with 10 mL of His-Binding buffer (Table 3) to rinse away any unbound bait protein. Untagged protein (prey protein) at 10 µM (1 mL) was loaded onto the same column. The column was incubated at 4 °C for 1 hr to allow the proteins to interact with one another and subsequently washed with 10 mL of His-Binding buffer (Table 3) to remove any unbound prey protein. The complex was eluted off the column with 10 mL of His-Elution buffer (Table 3). Flow through, wash and elution fractions were collected in 1 mL fractions and samples from each fraction were analyzed using sodium dodecyl sulfate

polyacrylamide gel electrophoresis (SDS-PAGE). Experiments were also done with N- and C-terminal truncated versions of NS1 to try to localize the rpL11 interaction surface of the protein.

Nuclear Magnetic Resonance

Nuclear magnetic resonance (NMR) was used to examine structural changes that occur to NS1 when it binds to rpL11. ^{15}N labeled NS1 was produced using auto-induction media supplemented with $^{15}NH_4Cl$[37]. NMR experiments were performed using the 800 MHz Varian instrument at the University of Connecticut Health Center (UCHC). Spectra were collected at 4 °C on protein samples in gel filtration buffer (Table 3; pH 6.5) with 10% D_2O. Chemical shifts of ^{15}N-labeled NS1 were monitored as a function of increasing concentration of rpL11. [^{15}N-^{1}H] HSQC spectra were obtained by holding NS1 at a concentration of 56 µM and adding increasing amounts of rpL11 from 0-155 µM. Spectra was analyzed using CcpNmr Analysis software[34].

Analytical Ultracentrifugation

Sedimentation velocity analytical ultracentrifugation (SV-AUC) was used to probe an interaction between NS1 and rpL11[3]. AUC experiments were performed using the Beckman XL-I analytical ultracentrifuge at 50,000 rpm and 4 °C in gel filtration buffer (Table 3) at the University of Connecticut. Sedimentation was observed using the absorbance optical system at 280-290 nm. The data were analyzed using DCDT+ 2.4.3 to obtain normalized sedimentation coefficient distributions, g(s*)[28,36].

GTP Hydrolysis Assay

The malachite green/ammonium molybdate colorimetric assay was used to measure the hydrolysis of GTP by detecting the release of free phosphate[16]. Steady state kinetic assays were done by mixing NS1 (5 uM) incubated with GTP (GE LifeSciences) over a concentration range

of 0.05-3 mM. The reactions were set up in 96-well plates with gel filtration buffer. A 30 µL-aliquot was removed at 0, 15, 30, 60 and 90 min and added to the malachite green/ammonium molybdate solution to stop the reaction. After a thirty min incubation at room temperature, the color development was measured at 660 nm by a SpectraMax i3X plate reader (Molecular Devices). Kinetic parameters were fit to the Michaelis-Menton equation with non-linear regression curve fitting using GraphPad Prism 7[10].

Results and Discussion

Pull-Down Assay

Based on the cellular localization of the protein and data gathered from siRNA knockdown of NS1 in *D. melanogaster*, we hypothesized that there was a functional interaction between NS1 and rpL11, which could be involved in 60S ribosome assembly[30]. A pull-down assay based on His-tag affinity chromatography was used to investigate the potential interaction between these two proteins. The His-tagged rpL11 was immobilized onto the nickel column which was then saturated with untagged NS1. The wash and elution fractions were analyzed using SDS-PAGE and visualized with coomassie stain. As shown in Figure 4, the hexa-His-tagged rpL11 is retained on the column until excess imidazole is added whereas the untagged protein does not bind the nickel column, most eluting in the first wash steps.

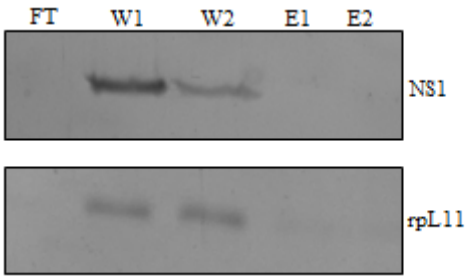

Figure 4. SDS-PAGE analysis of untagged proteins. Untagged NS1 and rpL11 proteins elute out in the wash fractions indicating no binding to the nickel column.

We began by testing complex formation between His-tagged rpL11 and untagged NS1 in the presence and absence of a 10-fold molar excess of GTP (Figure 5A and B). In both experiments, no protein was detected in the wash steps, but both rpL11 and NS1 were observed in the elution fractions. This suggested a guanine nucleotide independent binding event was occurring between NS1 and rpL11.

N- and C- terminal truncation proteins were used to localize the region of NS1 involved in complex formation. As mentioned previously, a structural characterization of NS1 by Tyler Daman showed that the termini of the protein are unstructured and therefore, well suited for partner binding. From Mr. Daman's analysis, the N-terminal IDR is defined as amino acid residues 1-135, and the C-terminal IDR is defined as amino acid residues 490-581. In Figure 5C, NS1 1-135 was in the wash fractions, and only His-tagged rpL11 was present in the elution fractions. This suggested that residues 1-135 of NS1 do not bind to rpL11. In contrast, un-tagged rpL11 co-eluted with His-tagged NS1 490-581 (Figure 5D). This was an interesting result because currently known binding partners, of NS protein family members, like MDM2 interact at the N-terminus, and few interactions at the C-terminus have been discovered[4]. Taken together,

these data suggest that a nucleotide independent interaction is occurring and complex formation is at least partially mediated by the C-terminal IDR of NS1.

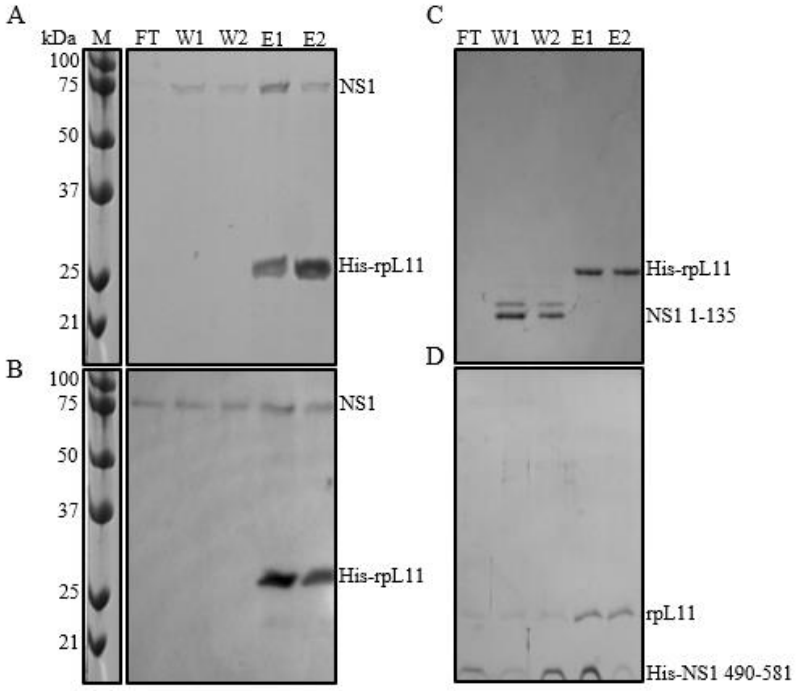

Figure 5. Affinity chromatography was used to assess the interaction of NS1 and rpL11. SDS-PAGE images of flow through (FT), wash 1 (W1), wash 2 (W2), elution 1 (E1), and elution 2 (E2) fractions from pull-down assays. **A.** Reaction between apo-NS1 and His-tagged rpL11. **B.** Reaction between NS1 and His-tagged rpL11 with the addition of 100 μM GTP. **C.** Reaction between NS1 1-135 and His-tagged rpL11. **D.** Reaction between rpL11 and His-tagged NS1 490-581.

Malachite Green Hydrolysis Assay

GTPases act as molecular switches in the cell for downstream signaling pathways[35]. When bound to GTP the switch is in the on state, and when GTP is hydrolyzed to GDP the switch is in the off state[35]. Some binding partners known as GTPase activating proteins (GAP) can stimulate catalytic activity by stabilizing the G-domain conformation necessary for hydrolysis[31]. The GTPase activity of the protein is also increased in the presence of guanine exchange factor (GEF) proteins that promote the release of GDP after the hydrolysis step[31]. The

malachite green phosphate detection assay was used to determine if rpL11 could stimulate catalytic activity of NS1.

Initial velocity rates for NS1 and the NS1 + rpL11 complex are shown in Figure 6. The intrinsic rate of GTP hydrolysis for NS1 was 24.6 hr^{-1} and has a K_m of 0.24 mM, which is similar to that measured previously (Table 4). The activity of NS1 in the presence of rpL11 was approximately the same, with k_{cat} and K_m values of 24.0 hr^{-1} and 0.19 mM, respectively (Table 4). Based on this result, rpL11 is not stimulating catalytic activity of NS1. Therefore, rpL11 does not act as a GAP or a GEF for NS1.

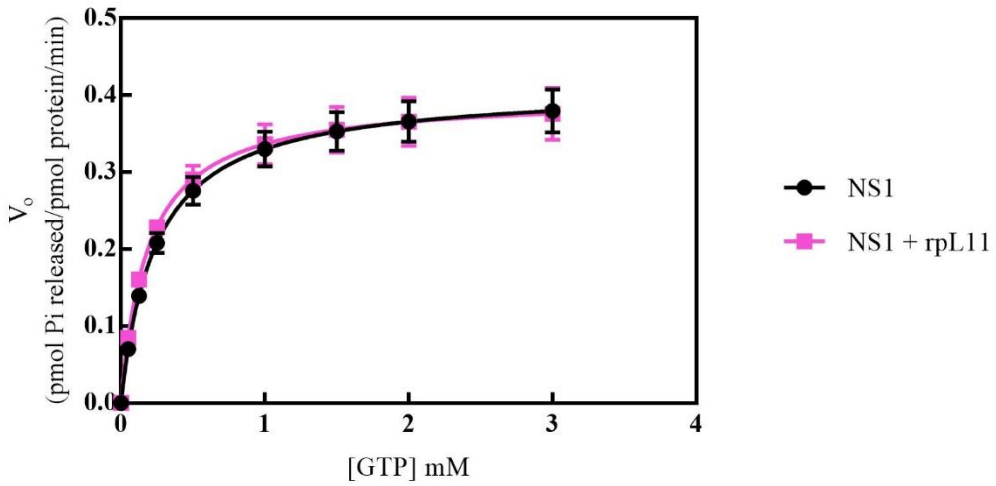

Figure 6. Steady state kinetic assays measuring the GTP hydrolysis rate of NS1 in the presence of rpL11. GTP (0.05-3 mM) hydrolysis activity of NS1 (5 µM) shown in black and NS1 with rpL11 (5 µM) shown in pink measured by the malachite green phosphate detection assay. The rate was calculated using the Michaelis-Menton equation and fit to a non-linear regression curve[11].

Table 4: Kinetic Parameters

Sample	V_{max} (pmol PO_4/pmol protein/min)	K_m (mM)	K_{cat} (hr^{-1})
NS1	0.41 ± 0.01	0.24 ± 0.02	24.6 ± 1.9
NS1 + rpL11	0.40 ± 0.01	0.19 ± 0.02	24.0 ± 2.3

Nuclear Magnetic Resonance

NMR was used to gather additional evidence that there was an interaction between NS1 and rpL11. NMR was chosen because it has been an invaluable tool in the study of IDPs and their interactions with other biological moieties, even in the case of transient binding events[10]. Based on our pull-down assays and owing to the size limitation of this technique, we decided to focus on the C-terminus of NS1. Figure 7 shows an example of the type of study we were trying to pursue. It is the [^{15}N-^{1}H] HSQC spectra of BASP1, an IDP which is characterized by narrow spectral ranges (Figure 7A)[38]. When IDPs interact with a binding partner, in this case MdmX, conformational ordering occurs resulting in significant chemical shifts by broadening or disappearing peaks in the NMR spectrum depending on the binding affinity of the interaction (Figure 7B)[8,26].

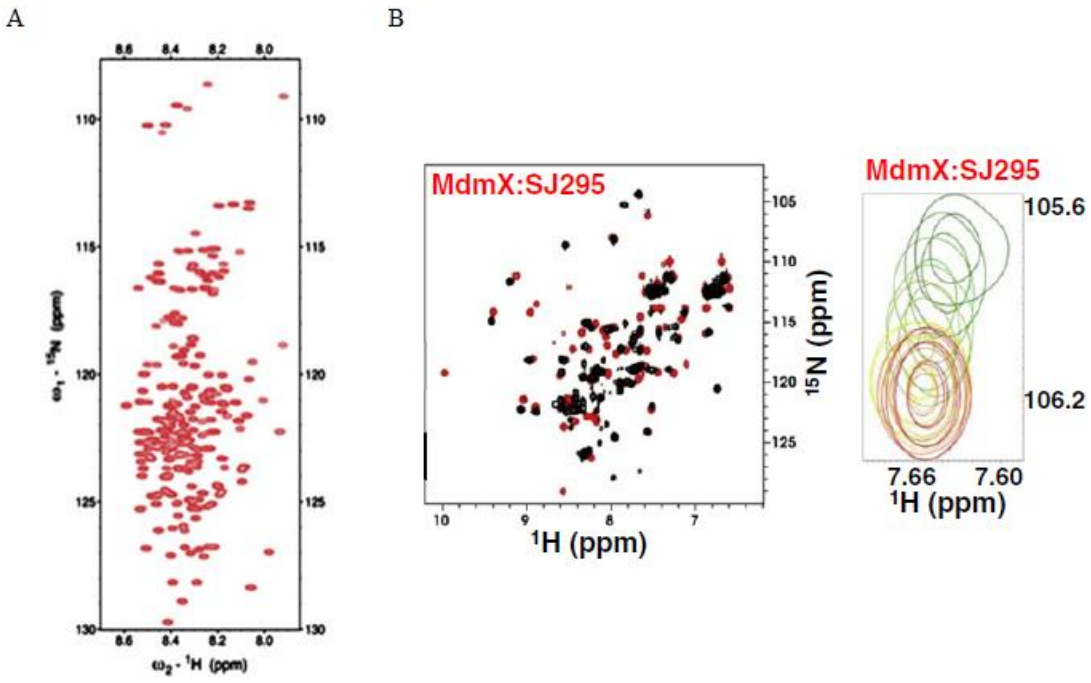

Figure 7. Characteristic [^{15}N-^{1}H] HSQC spectra of IDPs. A. The [^{15}N-^{1}H] HSQC spectrum of the IDP, BASP1 shows signal overlap and centrally collapsed peaks (Adapted from Konrat, et al.)[15]. **B.** On the left, a [^{15}N-^{1}H] HSQC spectrum shows significant chemical shifts upon binding to a partner (apo-MdmX is shown in black)[8]. On the right, a closer view of one of the peaks shifting as the binding event takes place is shown (Adapted from Grace, et al.)[8].

The molecular weight of NS1 490-581 protein is 14 kDa and so it is well suited for NMR studies. Figure 8A shows the [^{15}N-^{1}H] HSQC spectra of NS1 490-581. This spectrum is characteristic of an IDP where peaks are centrally collapsed due to lack of dispersion of proton resonances and severe signal-overlap. A titration [^{15}N-^{1}H] HSQC experiment was performed to identify chemical shifts in the NS1 490-581 spectrum due to conformational ordering upon binding to rpL11. Six spectra were collected from a titration of rpL11 spanning a concentration range of 25-155 µM. Figure 8B shows an overlay of the [^{15}N-^{1}H] HSQC spectra of NS1 490-581 and the rpL11 titrations. No large scale chemical shifts were observed.

Contrary to the pull-down assay these results suggest NS1 and rpL11 do not associate with one another. NMR, compared to the pull-down assay, is a more sensitive and a solution based technique providing us with compelling but also contradictory evidence about our system.

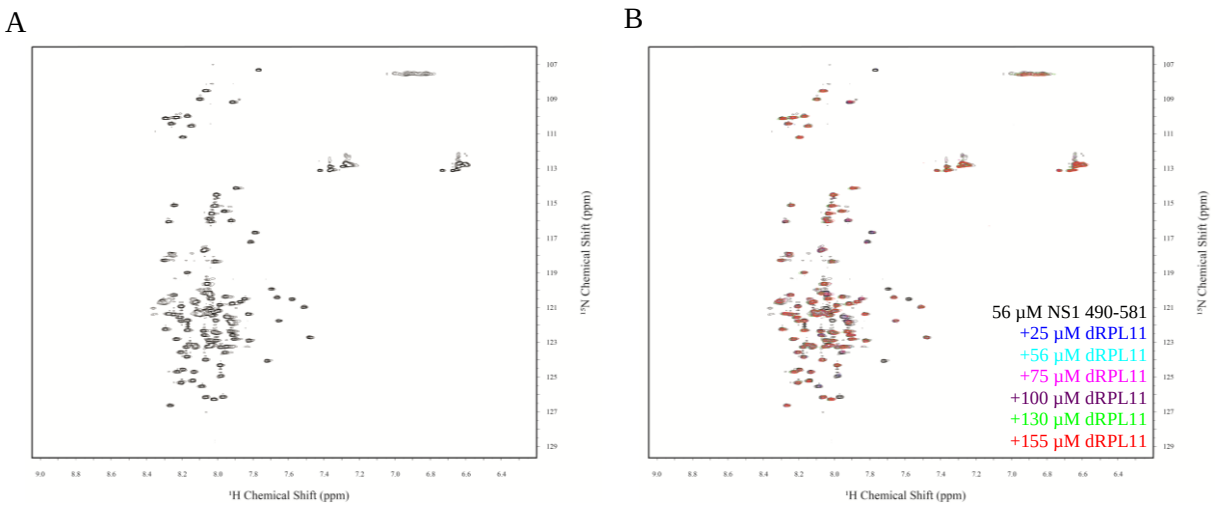

Figure 8. [^{15}N-^{1}H] HSQC spectra of NS1 and rpL11 A. [^{15}N-^{1}H] HSQC spectrum of NS1 490-581 (56 µM) at pH 6.5, 4°C. **B.** Overlay of [^{15}N-^{1}H] HSQC spectra of NS1 490-581 with rpL11 titrations (0-155 µM) at pH 6.5, 4°C.

Analytical Ultracentrifugation

Because the affinity assays and NMR data were not in agreement, analytical ultracentrifugation (AUC) was used to verify whether or not there was an interaction between NS1 and rpL11. Sedimentation equilibrium provides thermodynamic information by measuring concentration gradients, and sedimentation velocity provides hydrodynamic information by measuring the rate of sedimentation and diffusion[3]. While both sedimentation equilibrium and sedimentation velocity AUC (SV-AUC) can provide information on interacting systems, SV-AUC is more practical for interactions of proteins that are unstable[3].

For the reasons mentioned above, complex formation between NS1 and rpL11 was investigated using SV-AUC. The sedimentation coefficient distribution from a time derivative analysis is shown in Figure 9. Sedimentation coefficients were obtained for the individual proteins. The sedimentation coefficients for apo-NS1 and rpL11 are 1.79 S and 1.15 S, respectively (Figure 9). Sedimentation coefficients for apo-NS1 and rpL11 together were intermediate values of the individual sedimentation coefficients of NS1 and rpL11. These values were obtained from a concentration series of apo-NS1 and rpL11 together, starting at equimolar concentrations and going up to ~six-fold excess of rpL11 (Figure 9). The mixture also had a similar sedimentation coefficient when 100 µM GTP and 100 µM GDP were added (Figure 9). These results confirm there is no interaction.

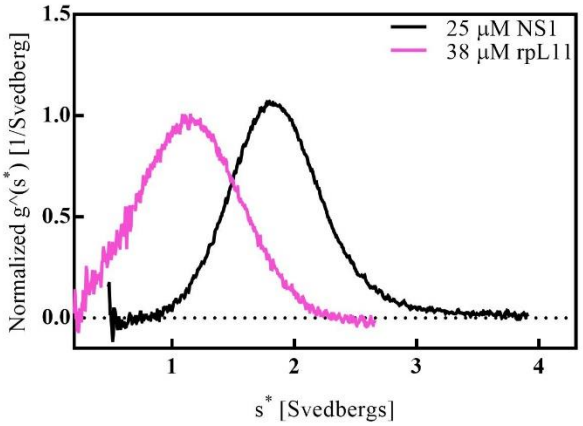

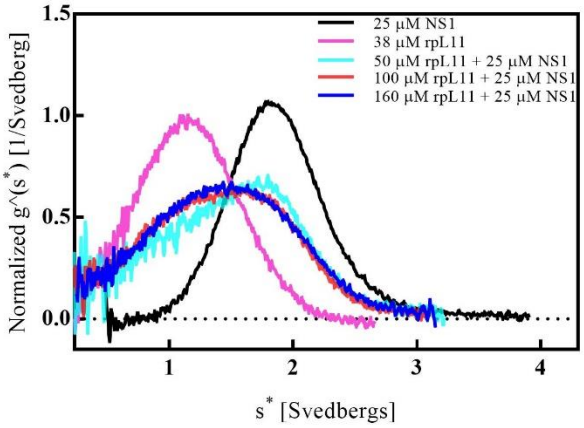

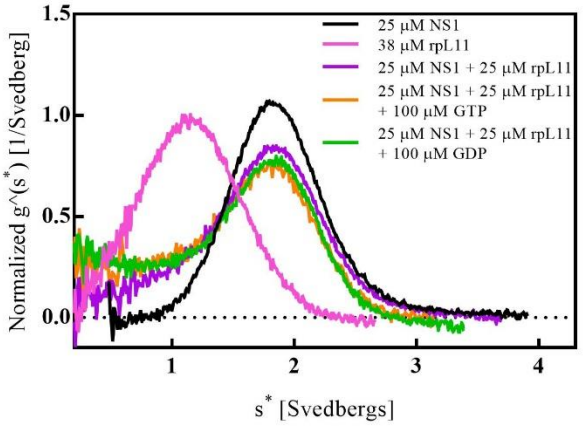

Figure 9. Sedimentation velocity analyses of NS1 and rpL11. Normalized g(s*) distribution for apo-NS1 with increasing concentrations of rpL11 (0-160 µM) as well as GTP- and GDP-bound NS1 with rpL11.

In conclusion, the sedimentation coefficients for the mixture of the proteins were smaller than the sedimentation coefficient of NS1 alone, which reveals the mixtures do not show complex formation. Experiments done in the presence of GTP yielded the same results. Therefore, the AUC data are in agreement with the NMR data suggesting there is no association of NS1 and rpL11.

Conclusions and Implications

Based on our study with the DiMario laboratory, we hypothesized that NS1 was somehow involved in an interaction with rpL11. Pull-down assays led us to believe there was an association occurring between the proteins. GTP hydrolysis assays showed rpL11 did not stimulate the catalytic activity of NS1 but this was not sufficient evidence to dismiss a potential interaction. We then moved to solution based methods to assess binding. Neither NMR nor AUC could detect any complex formation between NS1 and rpL11. Experiments were also done in the presence of GTP, but the results were the same.

Our conclusion is then, NS1 and rpL11 do not bind as purified components. However, this does not repudiate an interaction between NS1 and ribosome-bound rpL11. Another study done in the lab looked at an interaction between NS1 and rpL5, the other protein that forms the 5S rRNP complex. Similarly, the results showed NS1 and rpL5 do not interact either (*unpublished*, Tyler Daman). The CP in its entirety, rpL11, rpL5 and the 5S rRNA, may be required to facilitate the interaction.

As mentioned previously, both NS1 and rpL11 have pIs of 9.4 and 10.1, respectively. Although NS1 is basic overall, the C-terminal IDR has stretches of acidic residues, and the

surface of rpL11 is where the positively charged residues are enriched. Therefore, the interaction seen with the pull-down assay may have resulted from electrostatic interactions.

One major issue is, does NS1 actually bind to the Eukaryotic ribosome, specifically the *D. melanogaster* ribosome? This question, although simple in nature, is quite difficult to address. First of all, Eukaryotic ribosomes are structurally diverse due to the presence of protein and rRNA extension segments, and so there is no guarantee that a *D. melanogaster* protein would bind to a commercially available yeast ribosome. In an attempt to pursue these experiments, we obtained *D. melanogaster* cells from Dr. Barbara Mellone at the University of Connecticut with the intention to purify ribosomes. Although the purification was successful, we did not have enough ribosomes to perform a binding assay. The ribosome profile, shows the various particle species separated by a sucrose gradient based on density (Figure 10).

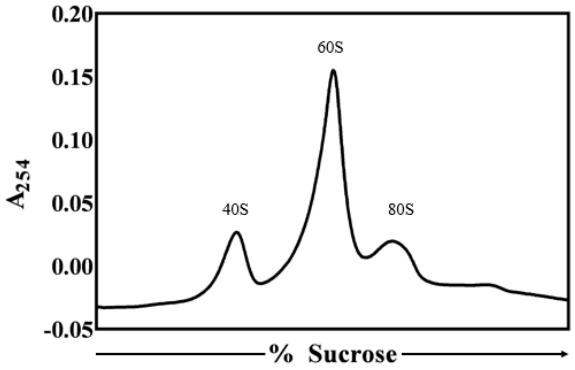

Figure 10. A Eukaryotic ribosome profile. This profile was generated on a 10-50% sucrose gradient. The least dense species, 40S particles, are found earliest in the elution profile while the densest species, 80S ribosomes are found latest in the elution profile.

Although no interaction was seen between NS1 and rpL11, further investigation is necessary. The evidence is very strong in support of NS1 regulation of 60S particle maturation. Additionally, this study has implications for finding cures for diseases and cancers that result from ribosomopathies[2].

Supplemental Material

Sucrose Density Gradient

Linear sucrose density gradients (10-50%) were prepared using five 500 mL solutions of 10%, 20%, 30%, 40%, 50% sucrose dissolved in 250 mM KCl, 20 mM Tris and 1 mM magnesium chloride ($MgCl_2$) (Buffer P). In descending order, 7 mL of each concentration were slowly added to a 42 mL plastic centrifuge tube (Beckman). Rubber stoppers were placed on top of each tube and the gradients were equilibrated for 2 hours.

Ribosome Purification

Ribosomes were purified from *D. melanogaster* Schneider 2 (S2) cells. The cells were provided by Dr. Barbara Mellone at the University of Connecticut. The cells were resuspended in Lysis Buffer (250 mM KCl, 20 mM Tris, pH 7.5, 1 mM magnesium chloride ($MgCl_2$), 0.1 % sodium-dodecyl-sulfate (SDS) and 1 % TritonX-100) and put on ice for 10 min. The cell lysate was clarified by centrifugation at 4 °C for 40 min at 15,000 *x g*. The cell lysate was then applied to a 1.1 M sucrose cushion in Buffer P and centrifuged at 250,000 *x g* for 16 hours at 4 °C. The supernatant was removed and the pellet (S100 fraction/total RNA) was resuspended in Buffer P. The S100 fraction was loaded onto a 10-50% sucrose density gradient prepared as described above and spun at 150,000 *x g* for 7 hr at 4 °C.

The sucrose density gradient was fractionated through a BioLogicTM Low Pressure chromatography system (Bio-Rad Laboratories). The washed 40S, 60S, and 80S ribosomes were quantified by A_{254}, where 1 40S A_{254} = 50 pmol, 1 60S A_{254} = 25 pmol, and 1 80S A_{254} = 20 pmol.

1. Anand, B., Verma, S. K., & Prakash, B. (2006). Structural stabilization of GTP-binding domains in circularly permuted GTPases: implications for RNA binding. *Nucleic Acids Research*, *34*(8), 2196–205.

2. Armistead, J., & Triggs-Raine, B. (2014). Diverse diseases from a ubiquitous process: The ribosomopathy paradox. *FEBS Letters*, *588*(9), 1491–1500.

3. Cole, J. L., Lary, J. W., P. Moody, T., & Laue, T. M. (2008). Analytical Ultracentrifugation: Sedimentation Velocity and Sedimentation Equilibrium. In *Methods in cell biology* (Vol. 84, pp. 143–179).

4. Dai, M.-S., Sun, X.-X., & Lu, H. (2008). Aberrant expression of nucleostemin activates p53 and induces cell cycle arrest via inhibition of MDM2. *Molecular and Cellular Biology*, *28*(13), 4365–76.

5. Daigle, D. M., Rossi, L., Berghuis, A. M., Aravind, L., Koonin, E. V, & Brown, E. D. (2002). YjeQ, an essential, conserved, uncharacterized protein from Escherichia coli, is an unusual GTPase with circularly permuted G-motifs and marked burst kinetics. *Biochemistry*, *41*(37), 11109–17.

6. Dinman, J. D. (2005). 5S rRNA: Structure and Function from Head to Toe. *International Journal of Biomedical Science : IJBS*, *1*(1), 2–7.

7. Du, X., Rao, M. R. K. S., Chen, X. Q., Wu, W., Mahalingam, S., & Balasundaram, D. (2006). The homologous putative GTPases Grn1p from fission yeast and the human GNL3L are required for growth and play a role in processing of nucleolar pre-rRNA. *Molecular Biology of the Cell*, *17*(1), 460–74.

8. Grace, C. R., Ban, D., Min, J., Mayasundari, A., Min, L., Finch, K. E., … Kriwacki, R. W. (2016). Monitoring Ligand-Induced Protein Ordering in Drug Discovery. *Journal of Molecular Biology*, *428*(6), 1290–303.

9. Henras, A. K., Plisson-Chastang, C., O'Donohue, M.-F., Chakraborty, A., & Gleizes, P.-E. (2015). An overview of pre-ribosomal RNA processing in eukaryotes. *Wiley Interdisciplinary Reviews: RNA*, *6*(2), 225–242.

10. Jensen, M. R., Ruigrok, R. W., & Blackledge, M. (2013). Describing intrinsically disordered proteins at atomic resolution by NMR. *Current Opinion in Structural Biology*, *23*(3), 426–435.

11. Johnson, K. A. (n.d.). A Century of Enzyme Kinetic Analysis, 1913 to 2013.

12. Jomaa, A., Stewart, G., Mears, J. A., Kireeva, I., Brown, E. D., & Ortega, J. (2011). Cryo-electron microscopy structure of the 30S subunit in complex with the YjeQ biogenesis factor. *RNA (New York, N.Y.)*, *17*(11), 2026–38.

13. Kim, D. J., Jang, J. Y., Yoon, H.-J., & Suh, S. W. (2008). Crystal structure of YlqF, a circularly permuted GTPase: Implications for its GTPase activation in 50 S ribosomal subunit assembly. *Proteins: Structure, Function, and Bioinformatics*, *72*(4), 1363–1370.

14. Konikkat, S., & Woolford, , John L. (2017). Principles of 60S ribosomal subunit assembly emerging from recent studies in yeast. *Biochemical Journal*, *474*(2), 195-214.

15. Konrat, R. (2014). NMR contributions to structural dynamics studies of intrinsically disordered proteins. *Journal of Magnetic Resonance (San Diego, Calif. : 1997)*, *241*(100), 74–85.

16. Lanzetta, P. A., Alvarez, L. J., Reinach, P. S., & Candia, O. A. (1979). An improved assay for nanomole amounts of inorganic phosphate. *Analytical Biochemistry*, *100*(1), 95–97.

17. Leipe, D. D., Wolf, Y. I., Koonin, E. V, & Aravind, L. (2002). Classification and evolution of P-loop GTPases and related ATPases. *Journal of Molecular Biology*, *317*(1), 41–72.

18. Li, C., Wen, A., Shen, B., Lu, J., Huang, Y., & Chang, Y. (2011). FastCloning: a highly simplified, purification-free, sequence- and ligation-independent PCR cloning method. *BMC Biotechnol*, *11*(1), 92.

19. Li, N., Chen, Y., Guo, Q., Zhang, Y., Yuan, Y., Ma, C., … Gao, N. (2013). Cryo-EM structures of the late-stage assembly intermediates of the bacterial 50S ribosomal subunit. *Nucleic Acids Research*, *41*(14), 7073–83.

20. Lin, T., Meng, L., Lin, T.-C., Wu, L. J., Pederson, T., & Tsai, R. Y. L. (2014). Nucleostemin and GNL3L exercise distinct functions in genome protection and ribosome synthesis, respectively. *Journal of Cell Science*, *127*(10).

21. Ma, H., & Pederson, T. (2008). Nucleophosmin is a binding partner of nucleostemin in human osteosarcoma cells. *Molecular Biology of the Cell*, *19*(7), 2870–5.

22. Meng, L., Hsu, J. K., & Tsai, R. Y. L. (2011). GNL3L depletion destabilizes MDM2 and induces p53-dependent G2/M arrest. *Oncogene*, *30*(14), 1716–26.

23. Mier, P., Pérez-Pulido, A. J., Reynaud, E. G., & Andrade-Navarro, M. A. (2017). Reading the Evolution of Compartmentalization in the Ribosome Assembly Toolbox: The YRG Protein Family. *PloS One*, *12*(1), e0169750.

24. Nunes, V. S., & Moretti, N. S. (2017). Nuclear subcompartments: an overview. *Cell Biology*

International, *41*(1), 2–7.

25. Pai, E. F., Krengel, U., Petsko, G. A., Goody, R. S., Kabsch, W., & Wittinghofer, A. (1990). Refined crystal structure of the triphosphate conformation of H-ras p21 at 1.35 A resolution: implications for the mechanism of GTP hydrolysis. *The EMBO Journal*, *9*(8), 2351–9.

26. Patil, A., & Nakamura, H. (2006). Disordered domains and high surface charge confer hubs with the ability to interact with multiple proteins in interaction networks. *FEBS Letters*, *580*(8), 2041–2045.

27. Pederson, T. (2011). The nucleolus. *Cold Spring Harbor Perspectives in Biology*, *3*(3).

28. Philo, J. S. (2006). Improved methods for fitting sedimentation coefficient distributions derived by time-derivative techniques. *Analytical Biochemistry*, *354*(2), 238–246.

29. Rao, M. R. K. S., Kumari, G., Balasundaram, D., Sankaranarayanan, R., & Mahalingam, S. (2006). A Novel Lysine-rich Domain and GTP Binding Motifs Regulate the Nucleolar Retention of Human Guanine Nucleotide Binding Protein, GNL3L. *Journal of Molecular Biology*, *364*(4), 637–654.

30. Rosby, R., Cui, Z., Rogers, E., deLivron, M. A., Robinson, V. L., & DiMario, P. J. (2009). Knockdown of the Drosophila GTPase nucleostemin 1 impairs large ribosomal subunit biogenesis, cell growth, and midgut precursor cell maintenance. *Molecular Biology of the Cell*, *20*(20), 4424–34.

31. Scheffzek, K., Ahmadian, M. R., & Wittinghofer, A. (1998). GTPase-activating proteins: helping hands to complement an active site. *Trends in Biochemical Sciences*, *23*(7), 257–62.

32. Scientific, T. (2010). Pulldown Assays in Thermo Scientific Pierce Protein Interaction

Technical Handbook. *Thermo Scientific Pierce Protein Interaction Technical Handbook*, *2*, 14–19.

33. Shin, D. H., Lou, Y., Jancarik, J., Yokota, H., Kim, R., & Kim, S.-H. (2004). Crystal structure of YjeQ from Thermotoga maritima contains a circularly permuted GTPase domain. *Proceedings of the National Academy of Sciences of the United States of America*, *101*(36), 13198–203.

34. Skinner, S. P., Goult, B. T., Fogh, R. H., Boucher, W., Stevens, T. J., Laue, E. D., & Vuister, G. W. (2015). Structure calculation, refinement and validation using CcpNmr Analysis. *Acta Crystallographica Section D: Biological Crystallography*, *71*, 154–161.

35. Sprang, S. R. (1997). G PROTEIN MECHANISMS:Insights from Structural Analysis. *Annual Review of Biochemistry*, *66*(1), 639–678.

36. Stafford, W. F. (1992). Boundary analysis in sedimentation transport experiments: A procedure for obtaining sedimentation coefficient distributions using the time derivative of the concentration profile. *Analytical Biochemistry*, *203*(2), 295–301.

37. Studier, F. W. (2005). Protein production by auto-induction in high-density shaking cultures. *Protein Expression and Purification*, *41*(1), 207–234.

38. Tamiola, K., Acar, B., & Mulder, F. A. A. (2010). Sequence-specific random coil chemical shifts of intrinsically disordered proteins. *Journal of the American Chemical Society*, *132*(51), 18000–3.

39. Tsai, R. Y. L., & Meng, L. (2009). Nucleostemin: a latecomer with new tricks. *The International Journal of Biochemistry & Cell Biology*, *41*(11), 2122–4.

40. Uversky, V. N., Oldfield, C. J., Midic, U., Xie, H., Xue, B., Vucetic, S., … Dunker, A. K. (2009). Unfoldomics of human diseases: linking protein intrinsic disorder with diseases. *BMC Genomics*, *10 Suppl 1*(Suppl 1), S7.

41. Wilson, D. N., & Doudna Cate, J. H. (2012). The structure and function of the eukaryotic ribosome. *Cold Spring Harbor Perspectives in Biology*, *4*(5), a011536.

42. Zhang, Y. (2008). I-TASSER server for protein 3D structure prediction. *BMC Bioinformatics*, *9*(1), 40.

43. Zhu, Q., Meng, L., Hsu, J. K., Lin, T., Teishima, J., & Tsai, R. Y. L. (2009). GNL3L stabilizes the TRF1 complex and promotes mitotic transition. *The Journal of Cell Biology*, *185*(5), 827–39.